The gas-phase structure determination of α-pinene oxide: An endo-cyclic epoxide of atmospheric interest

E M Neeman, N. Osseiran, T R Huet

Accepted to J. Chem. Phys. 10.1063/5.0147909

The gas-phase structure determination of α-pinene oxide: an endo-cyclic epoxide of atmospheric interest

E. M. Neeman*[a], N. Osseiran [a] and T. R. Huet* [a]

[a] Univ. Lille, CNRS, UMR 8523 - PhLAM - Physique des Lasers Atomes et Molécules, F-59000 Lille, France.

* Corresponding authors: Elias.Neeman@univ-lille.fr; Therese.Huet@univ-lille.fr

Abstract

Gas-phase rotational spectra of α-pinene oxide have been recorded using a chirped-pulse Fourier transform microwave spectrometers in the 6-18 GHz frequency range. Parent species and all heavy atom isotopologues ^{13}C and ^{18}O have been observed in their natural abundance. The experimental rotational constants of all isotopic species observed have been determined and used to obtain the substitution (r_s) and the effective (r_0) structures of the most stable conformer of α-pinene oxide. Calculations using the density functional theory B3LYP, M06-2X and MN15-L as well as the ab initio method MP2 level of theory were carried out to check their performance against experimental results. The structure of the heavy atom's skeleton of α-pinene oxide has been compared to α-pinene and has shown that epoxidation does not affect overmuch the structure of the bicycle, validating its robustness. Furthermore, structural features have been compared to other bicyclic molecules nopinone and β-pinene.

Introduction

Monoterpenes ($C_{10}H_{16}$) are biogenic organic volatile compounds (BVOC) emitted in the atmosphere from vegetation and represent a major source of reactive biogenic species. On a global scale, plants emit the equivalent to 10^{14} g.yr^{-1} of monoterpenes which represent 11% of the total BVOCs emission.[1,2] Those can react rapidly with other atmospheric oxidants such as O_3, OH and NO_x radicals to form low volatile compounds making them among the most important class of secondary organic aerosols (SOA) precursors. SOA represent a source of uncertainty for climate simulations since their formation and evolution mechanisms remain poorly understood and deserve more attention.[3] They play an important role in the global climate[4] and regional air quality since they degrade visibility by absorbing and reflecting solar radiation, or by modifying cloud formation.[5] They affect human health.[6,7]

α-pinene is the most abundant monoterpene in the atmosphere and its oxidation leads to the formation of different class[8] of oxygenated monoterpenoids that are involved in the formation of atmospheric SOA. Among the formed species is α-pinene oxide,[9] which is formed in high yield from the direct reaction of ozone with α-pinene.[10,11] Recently, studies have shown that the reaction of epoxides with sulfuric acid is kinetically preferred over the reaction of alcohols with sulfuric acid for the formation of organosulfates.[12] α-pinene oxide (APO), $C_{10}H_{16}O$, 2,7,7-Trimethyl-3-oxatricyclo[4.1.1.02,4]octane is an endo-cyclic epoxide which has been observed to participate in the formation of organosulfates under atmospheric conditions.[12] Apart their role in atmospheric chemistry, terpenes and their oxidation products are also the essential building blocks in the food flavour, pharmaceutical and fragrance industries.[13] For that reason α-pinene

oxide is used to produce several compound highly valuable fragrance and/or pharmaceutical ingredients via an acid-catalysed mechanism.[14] Recent microwave studies supported by quantum chemical calculations on bicyclic monoterpenes[15–19] have shown the structural characteristics between similar bicyclic molecules with different functional group. For example, the structure of β-pinene is quasi-unchanged upon oxidation to nopinone (Figure 1).[16]

The introduction of high-resolution broadband microwave spectroscopy[20,21] (CP-FTMW) permitted an efficient search for different species present in the supersonic jet. This technique allows the collection at once of a large portion of the rotational spectrum of a molecule. In other words, every frequency element of the whole acquired spectrum is collected in every shot of the spectrometer. Consequently, it facilitates the identification of spectral patterns and reduces acquisition time.

In this study, we used a new CP-FTMW spectrometer recently constructed at Lille. The recorded spectra, of parent and isotopologue species of APO, have been analyzed and the rotational molecular parameters have been obtained. Their values have been used to determine the structure of the heavy atom skeleton using substitution (r_s) and ground state (r_0) methods. A

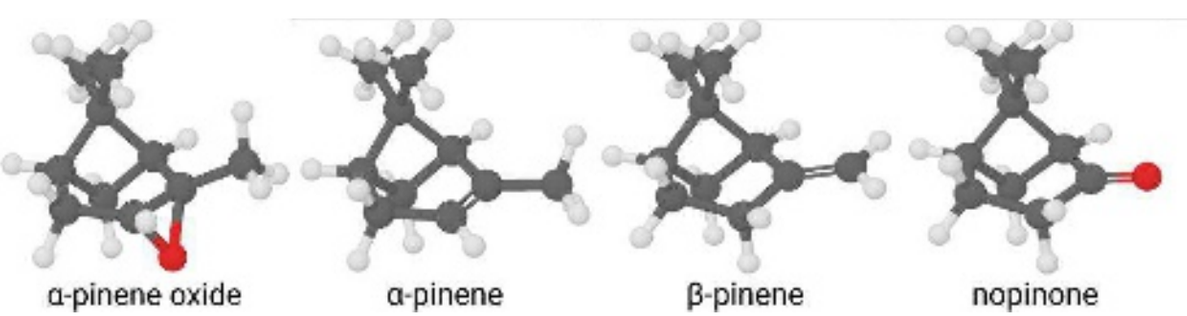

Figure 1. 3-D structures of the four molecules α-pinene oxide, α-pinene, β -pinene and nopinone

comparison with similar bicyclic terpenoids such as α-pinene, β-pinene and nopinone has been made. It highlights the structure features between those related molecules.

Methods

Quantum chemical calculations

Quantum chemical calculations were performed using the Gaussian 16 software package.[22] The structures of APO have been optimised using Møller–Plesset second order perturbation theory (MP2) [23] and the DFT method B3LYP,[24,25] M06-2X,[26] and MN0-L15.[27] Pople split-valence triple-zeta basis set augmented with diffuse and polarization functions on all atoms basis set (6-311++G(d,p)) were used.[28] The set of equilibrium molecular parameters has been obtained from the structure, such as rotational constants (A, B, C), quartic centrifugal distortion parameters (D_J, D_{JK}, D_K, d_1, d_2) and permanent electric dipole moment components (μ_a, μ_b, μ_c).

Experimental

The jet-cooled pure rotational spectra (6–18 GHz) of APO were recorded on the recently developed CP-FTMW spectrometer, in Lille.[29] A 65 GSa/s arbitrary waveform generator (AWG, Keysight M8195A) generates a fast chirp microwave pulse spanning 1-5 μs and varying linearly in frequency sweep. A 300 W traveling wave tube amplifier (Instruments for Industry, GT186-300) amplifies the microwave pulse in the 6-18 GHz region. It is coupled into a vacuum chamber via a standard horn antenna (ATM 650-442-C3), where it polarizes all transitions in the molecular sample produced with up to three pulsed valves (Parker IOTA ONE). A second horn antenna is used to detect the free induction decay signals (FIDs) emitted by the molecular ensemble as

response to the microwave excitation. A pin diode limiter (AMS/COBHAM ACLM-4537) protects the detection branch of the electronics from accidental damage. Then the collected FIDs are further amplified by a low noise amplifier (MITEQ amplifier JS42-06001 800-20-10P). A digital oscilloscope (160 GSa/s, 63 GHz hardware bandwidth, Keysight DSOZ634A) collects the amplified rotational FIDs in the time domain. A microwave single-pole single-throw switch (SPST, ATM S1517D) is used to protect the oscilloscope. To enable a coherent system all the electronic components are phase-locked to the same 10 MHz rubidium frequency standard clock (SRS FS725). A digital pulse delay generator (Berkeley Nucleonics Corp Model 577) manages the sequences. The FIDs can then be coadded, and the final molecular FID transformed on the computer to the frequency domain using a program written in Python and including different window function options such as Kaiser-Bessel, Bartlett or Hann.

APO (98%) was purchased as liquid sample from Merck and was used without any further purification. The sample was placed inside the reservoir of a pulsed nozzle and heated to about 363 K and mixed with a carrier gas (Ne or Ar) at stagnation pressure of 2 bar. The sample was then injected inside the vacuum chamber at a repetition rate of 2 Hz. A molecular pulse of about 900 µs is used to create the supersonic jet expansion. Chirp microwave pulses of 4 µs were applied with a delay of about 400-500 µs with respect to the start of the molecular pulse. Up to 8 FIDs per gas pulse were collected for 20 µs using the digital oscilloscope and then Fourier-transformed in the Kaiser-Bessel windows function. As microwave radiation is perpendicular to the supersonic jet in our setup, the FWHM of the observed lines is estimated to be ~100 kHz in the present spectra. In addition to the CP-FTMW spectra, we performed a few measurements for

the APO ^{18}O isotopologue to record more lines by using the Lille Fabry–Pérot (FP) cavity. This experimental set-up has been described in details elsewhere.[15,30]

Results

Calculated structures

The only degree of freedom in APO is the position of the epoxide in the molecule. It leads to two possible configurations, presented in Figure 2. The calculated rotational parameters of the lowest energy structure are reported in Table I. The second conformer is very high in energy (≈18 kJ/mol, ≈ 15 kJ/mol, 20 kJ/mol at the MP2/6-311++G(d,p)) and is not detectable in the supersonic expansion. Its rotational parameters are given in the supplementary materials, together with the Cartesian coordinates of the two conformers.

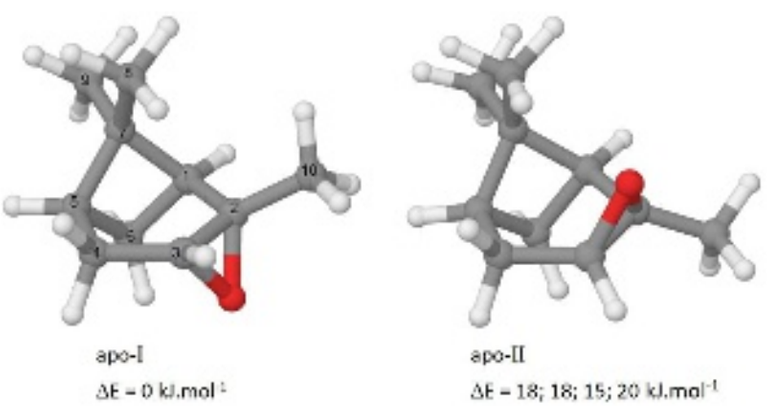

Figure 2. Equilibrium structure, of the possible conformer of α-pinene oxide with the numbering of carbons skeleton (left), and of the less stable conformer (right). They differ by the position of the epoxide group. ΔE is relative electronic energy in kJ.mol^{-1} calculated at MP2; M06-2X; B3LYP; MN15-L levels respectively, with 6-311++G(d,p) basis set.

Broadband spectrum

The broadband rotational spectrum of APO is shown in Figure 3. It is very dense and shows a series of intense lines with many weaker lines.

According to theoretical calculations, APO is an asymmetric prolate rotor with a Ray's asymmetry parameter ($\kappa = (2B - A - C)/(A - C)$) value equal to -0.67. The main component of the dipole moment lies along the *a*-inertial axis. A set of intense lines was observed in the recorded broadband spectrum and identified as a-type R-branch. Indeed $(J+1)_{0,J+1} \leftarrow J_{0,J}$ and $(J+1)_{1,J+1} \leftarrow J_{1,J}$ lines spaced approximately by B + C were easily identified. Following iterative fittings and predictions, c-type and b-type R-branches and Q-branches transitions were then

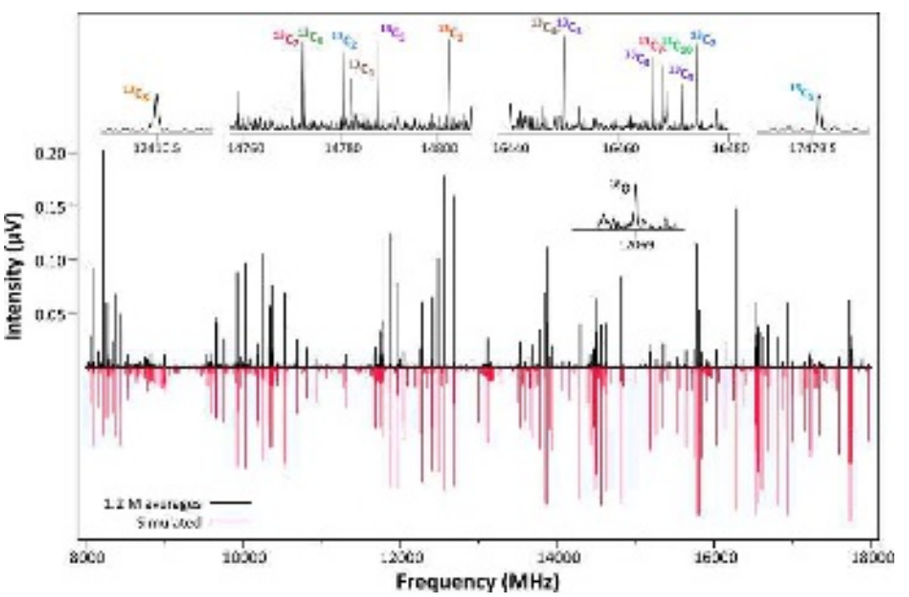

Figure 3. The broadband spectrum of α-pinene oxide recorded in the 8-18 GHz frequency range using Ar as carrier gas, together with a simulated spectrum at 5 K. Signals from all the isotopologues (^{13}C, ^{18}O) are presented in the upper part of the spectrum, from the broadband spectrum.

Table I. Experimental spectroscopic parameters for the ground state of α-pinene oxide compared with those predicted from quantum chemical calculations.

	Parent species				
	Experimental	**MP2**[e]	**B3LYP**[e]	**M06-2X**[e]	**MN15-L**[e]
A[a]	1726.71952(16)	1730.1 (-0.2%)	1722.6 (-0.2%)	1735.1 (-0.5%)	1710.9 (0.9%)
B[a]	1092.35191(11)	1096.3 (-0.4%)	1080.6 (1.1%)	1100.4 (-0.7%)	1088.9 (0.3%)
C[a]	968.23479(12)	971.5 (-0.3%)	959.0 (1.0%)	974.6 (-0.7%)	962.4 (0.6%)
$\mathbf{D_J}$[a]	0.03793(68)	0.0363	0.0363	0.0361	0.0338
$\mathbf{D_K}$[a]	0.05316(72)	0.0556	0.0560	0.0569	0.0541
$\mathbf{D_{JK}}$[a]	-0.01782(63)	-0.0191	-0.0182	-0.0201	-0.0177
$\mathbf{d_1}$[a]	0.006077(79)	0.00613	0.00619	0.00629	0.00526
$\mathbf{d_2}$[a]	0.0254(13)	0.0272	0.0250	0.0271	0.0265
$\lvert\mu_a\rvert$[b]	Observed	1.6	1.5	1.5	1.4
$\lvert\mu_b\rvert$[b]	Observed	0.9	0.9	1.0	0.8
$\lvert\mu_c\rvert$[b]	Observed	1.1	1.1	1.1	1.0
N[c]	567	-	-	-	-
σ[d]	11	-	-	-	-

[a] A, B, C are the rotational constants given in MHz; D_J, D_{Jk}, D_k, d_1 and d_2 are the quartic centrifugal distortion given in kHz; [b] μ_a, μ_b, μ_c are the components of the electric dipole moment in D; [c] Number of fitted transitions; [d] rms deviation of the fit in kHz; [e] 6-311++G(d,p) basis set.

identified in the spectrum. A total of 567 transitions were fitted together using SPFIT/SPCAT suite of program[31] with a Watson's semi-rigid rotor Hamiltonian[32] in the I^r representation and in the S-reduction. All the observed lines of APO are available in the supplementary material.

The values of the rotational constants obtained from the fit for the parent species are reported in Table I. After cleaning the rotational spectra from the assigned lines of APO small lines were identified as belonging to the ten possible ^{13}C isotopologues in their natural abundance (1.1%) and about four very small lines were assigned to ^{18}O isotopologue in its natural abundance (0.2%). Further experiments were performed using the FP-FTMW spectrometer of Lille to record more line transitions for the isotopologue ^{18}O in its natural abundance. The corresponding rotational constants are reported in Table II.

Table II. Experimental rotational constants for the ^{13}C and ^{18}O isotopologues of APO-I. The numbering of carbon atoms refers to Figure 1.

	$^{13}C1$	$^{13}C2$	$^{13}C3$	$^{13}C4$	$^{13}C5$	$^{13}C6$
A (MHz) [a]	1720.4015(49)	1724.9625(10)	1721.4047(14)	1707.049(15)	1717.803(25)	1709.9532(43)
B (MHz)	1090.16193(47)	1089.02183(56)	1086.35389(42)	1089.47355(69)	1090.13622(79)	1088.07344(70)
C (MHz)	967.95785(42)	965.28418(37)	964.32972(31)	964.06316(66)	963.81451(62)	965.52835(67)
σ (kHz) [b]	14.0	13.7	14.0	9.9	11.1	11.2
N [c]	22	22	26	15	14	13
	$^{13}C7$	$^{13}C8$	$^{13}C9$	$^{13}C10$	^{18}O [d]	
A (MHz) [a]	1726.1856(16)	1708.2239(10)	1723.6656(51)	1706.8298(40)	1720.6760(39)	
B (MHz)	1088.32659(49)	1084.53754(90)	1074.93691(67)	1084.34373(79)	1071.56547(11)	
C (MHz)	964.92859(43)	963.02249(71)	954.49869(56)	955.88732(43)	951.22344(10)	
σ (kHz) [b]	14.4	13.1	14.7	10.9	1.3	
N [c]	32	19	18	13	12	

[a] *A, B, C* are the rotational constants given in MHz; the quartic centrifugal distortion constants were kept fixed to the parent species values; [b] rms deviation of the fit in kHz; [c] Number of fitted transitions; [d] Line transitions from FP-FTMW were fitted together.

To benchmark the performance of theoretical calculation, we compared the experimental rotational constants with those predicted from theory using density functional theory, with the B3LYP, M06-2X and MN15-L functionals, and *ab initio* calculations at MP2 level of theory all used with Pople's 6-311G++(d,p) basis set. From the data in Table I, all methods predict very close rotational constants. Meanwhile, the best agreement with the experimental rotational constants is provided by calculations at the MP2/6-311++G(d,p) level which is better than 0.4%.

Molecular structure

The tricyclic structure of APO seems very rigid, as reflected by the small values of the centrifugal distortion parameters. As in the case of similar molecules,[15,16,18] no evidence of splitting due to internal rotation of the methyl group was observed in the rotational spectrum. Further theoretical calculations at the B3LYP/6-311++(d,p) level have been performed to calculate the barrier height of the three methyl groups in APO. Those barrier heights were found to be very

high (875 cm^{-1} for C_{10}, 860 cm^{-1} for C_9, 1040 cm^{-1} for C_8) similar to those calculated for α- pinene,[15] β-pinene and nopinone.[14]

The obtained molecular parameters for the parent species and all isotopologues, allows the determination of an experimental gas phase structure of the heavy atom's skeleton of APO. Indeed since the rotational constants are linked to the atomic distribution in the molecule it is possible to calculate an experimental structure of the heavy atom skeleton using the substitution structure (r_s) based on Kraitchman's equations,[33] and by estimate their Costain uncertainties[34] from vibration-rotation effects. Structural parameters from the r_s structure, are given in Table III. The determined r_s coordinates are reported along with their calculated uncertainties in electronic supplementary materials.

It was also possible to determine the ground state effective geometry (r_0) of heavy atom substitution by fitting the molecular geometry directly to all observed moments of inertia, and by taking CH bond lengths and CCH angles from the *ab initio* MP2 calculations which gives the better agreement with experimental rotational constants. The obtained results are also presented in the Table III. The experimental structure of the skeleton atoms is also compared to the two best theoretical MP2/6-311++G(d,p) and M06-2X/6-311++G(d,p) calculations.

Discussion

Based on data from all isotopologues, both r_s and r_0 structures have been determined and compared with theoretical values and those of a few related species such as α-pinene, β-pinene and nopinone. By comparing the obtained structures, some of molecular parameters obtained

from r_s differ with those obtained from r_0 and theoretical values. Those parameters involve atoms that are close to the principal axis. Kraitchman's method provides the absolute values of coordinates for the substituted atoms, in the center of mass system for the parent species, using differences in moments of inertia for the parent and singly substituted molecules. The accuracy of these coordinates is significantly reduced and the uncertainties in atom coordinates are typically magnified when the substituted atom lies close to a principal axis or the center of mass. This is the case for example of the C1 atom and therefore molecular parameters involving C1 are affected. For that reason, and to compare the structures of related bicyclic molecules we use the r_0 structures.

The structure of APO is very similar to the structure of α-pinene, meanwhile a few features can be noticed from the comparison of their r_0 structures. The main difference involves the bond length C_3C_2 which is double bond in the α-pinene and consequently shorter than in the APO. Concerning the angles, their values in both molecules are very similar. In the case of dihedral angles, $C_4C_3C_2C_1$ and $C_2C_3C_4C_5$ are close to 0° in both cases. The other dihedral angles have relativity very close values. The main differences involve $C_{10}C_2C_3C_1$ and $C_{10}C_2C_3C_4$ dihedral angles that are close to 180° in the case of α-pinene, and the value decrease of about 30° in the APO molecule. This is due to the presence of the epoxide functional group linked to the C_3 and C_2 atoms. This also could be observed in the value of the $C_2C_1C_6$ angle which is bigger in the case of APO than in the α-pinene by about 4°. The presence of the epoxide forces the 5-members ring to open further reshaping its structure. The other structure parameters of APO are close to their corresponding parameters in the α-pinene suggesting that the overall structure in the gas phase

is very similar in both molecules. This demonstrates once again the rigidity of this type of bicyclic molecules despite the fact of epoxidation and the presence of a third cycle, α-pinene oxide conserves a similar structure to α-pinene.

The gas phase structure of APO can be compared also with the two other similar molecules such as the pinene isomer β-pinene and its oxidation product nopinone. The bond lengths are very close in the three molecules and again except for C_3C_2 induced by the presence of the epoxide group. We could note, from the comparison of the r_0 structures, significant differences in their dihedral angles. It can be observed that the $C_2C_3C_4C_5$, $C_4C_3C_2C_1$and $C_3C_4C_5C_7$ dihedral angles are smaller in the case of APO than in the β-pinene and nopinone. The $C_3C_4C_5C_6$ and $C_3C_4C_5C_7$ dihedral angles are bigger in the APO than in β-pinene and nopinone. Surprisingly, the $C_{10}C_2C_3C_4$ dihedral angle is closer to β-pinene than to α-pinene, but again $C_{10}C_1C_2C_3$ is completely different from β-pinene. The presence of the epoxide tilts the structure of this $C_{10}C_1C_2C_3$ dihedral angle of about 30°.

Table III. Comparison of the geometrical parameters (lengths/Å and angles/°) values determined experimentally and theoretically for the heavy atoms of α-pinene oxide, and with those of other related molecules α-pinene, β-pinene and nopinone.

	α-pinene oxide (APO-I)				α-pinene [a]	β-pinene [b]	nopinone [b]
		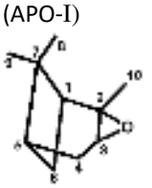			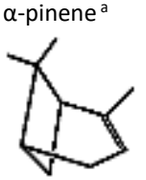	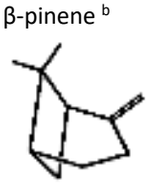	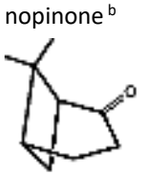
Parameter	r_s	r_0	M06-2X [c]	MP2 [c]	r_0	r_0	r_0
$r(C_3C_2)$	1.461(6)	1.475(12)	1.471	1.472	1.349(15)	1.513(10)	1.525(10)
$r(C_4C_3)$	1.533(5)	1.521(8)	1.521	1.519	1.509(7)	1.546(7)	1.544(8)
$r(C_4C_5)$	1.518(8)	1.536(10)	1.534	1.535	1.545(8)	1.530(12)	1.533(13)
$r(C_5C_7)$	1.560(5)	1.571(11)	1.564	1.566	1.558(10)	1.546(10)	1.545(11)

$r(C_1C_7)$	1.641(29)	1.576(14)	1.569	1.571	1.567(12)	1.561(15)	1.564(18)
$r(C_2C_{10})$	1.514(3)	1.511(6)	1.503	1.504	1.500(6)	1.339(5)	-
$r(C_6C_5)$	1.557(10)	1.551(11)	1.548	1.551	1.554(12)	1.563(13)	1.559(13)
$r(C_7C_8)$	1.557(16)	1.537(18)	1.526	1.526	1.527(13)	1.538(16)	1.539(18)
$r(C_7C_9)$	1.523(8)	1.530(11)	1.529	1.530	1.538(8)	1.526(9)	1.526(10)
$r(C_1C_2)$	1.413(30)	1.507(13)	1.526	1.523	1.512(16)	1.491(13)	1.499(13)
$r(C_1C_6)$	1.577(10)	1.557(8)	1.546	1.549	1.565(7)	1.556(8)	1.554(8)
$r(C_2O)$	1.442(3)	1.445(7)	1.427	1.450	–	–	–
$r(C_3O)$	1.442(4)	1.445(6)	1.426	1.448	–	–	–
$\angle(C_2C_3C_4)$	117.2(2)	117.6(3)	117.8	117.9	119.5(4)	113.4(2)	114.1(2)
$\angle(C_5C_4C_3)$	111.4(2)	111.6(2)	111.3	111.3	110.4(3)	111.3(3)	111.5(4)
$\angle(C_4C_5C_7)$	112.3(5)	111.6(6)	111.4	111.4	110.7(6)	110.8(6)	111.9(10)
$\angle(C_1C_7C_5)$	85.5(5)	85.4(7)	85.1	85.2	85.4(6)	85.7(5)	86.6(8)
$\angle(C_{10}C_2C_3)$	121.7(4)	121.5(8)	122.1	122.1	123.7(12)	122.5(5)	–
$\angle(C_6C_5C_4)$	109.5(3)	109.2(4)	109.2	109.2	108.0(6)	108.9(5)	108.4(6)
$\angle(C_8C_7C_5)$	117.4(11)	118.2(13)	118.8	118.9	119.4(10)	119.6(8)	118.8(12)
$\angle(C_9C_7C_1)$	116.4(14)	112.8(14)	111.9	111.8	111.6(8)	111.3(10)	112.1(13)
$\angle(C_{10}C_2C_1)$	116.8(3)	117.5(7)	117.1	117.2	119.4(11)	123.3(6)	–
$\angle(C_8C_7C_9)$	107.0(5)	107.7(7)	108.1	108.2	108.1(6)	108.7(6)	108.0(8)
$\angle(C_8C_7C_1)$	117.0(6)	119.4(6)	119.6	119.7	119.1(5)	118.0(5)	117.5(6)
$\angle(C_9C_7C_5)$	112.7(5)	112.0(8)	111.8	111.7	111.9(7)	112.0(6)	112.7(9)
$\angle(C_5C_6C_1)$	87.8(4)	86.5(3)	86.4	86.4	85.6(3)	86.3(4)	86.5(4)
$\angle(C_6C_5C_7)$	86.4(8)	86.9(9)	87.6	87.5	87.8(6)	88.1(6)	87.5(9)
$\angle(C_2C_1C_6)$	113.5(12)	110.3(7)	109.6	109.7	106.5(7)	109.3(6)	108.8(8)
$\angle(C_1C_2C_3)$	116.3(4)	114.7(4)	114.2	114.2	116.9(5)	114.2(4)	115.0(4)
$\angle(C_2C_1C_7)$	109.8(6)	109.2(8)	108.8	108.6	110.2(10)	108.9(6)	108.2(3)
$\angle(C_6C_1C_7)$	83.0(12)	86.7(7)	87.6	87.4	87.1(6)	87.0(5)	86.9(7)
$\angle(OC_2C_3)$	59.6(2)	59.3(4)	59.0	59.4	–	–	–
$\angle(OC_3C_2)$	59.6(2)	59.3(4)	58.9	59.6	–	–	–
$\angle(C_2OC_3)$	60.9(3)	61.4(5)	62.1	61.1	–	–	–
$\angle(OC_2C_{10})$	114.3(1)	114.7(3)	115.5	114.9	–	–	–
$\angle(OC_2C_1)$	115.0(5)	116.1(7)	116.1	116.0	–	–	–
$\angle(OC_3C_4)$	117.8(2)	117.8(4)	118.1	117.8	–	–	–
$\angle(C_2C_3C_4C_5)$	-1.0(4)	-1.4(9)	-1.1	-1.5	1.9(18)	21.6(9)	16.1(9)
$\angle(C_4C_3C_2C_1)$	-2.9(8)	-0.8(9)	-0.7	-0.5	-1.3(24)	23.7(10)	-18.8(11)
$\angle(C_4C_5C_7C_1)$	78.9(11)	81.5(10)	82.7	82.6	80.6(7)	82.7(8)	83.8(7)
$\angle(C_3C_4C_5C_7)$	-45.2(8)	-45.2(10)	-46.1	-45.7	-48.5(10)	-58.6(9)	-55.5(8)
$\angle(C_3C_4C_5C_6)$	49.0(3)	49.1(4)	49.0	49.3	46.1(7)	36.6(5)	40.1(5)
$\angle(C_4C_5C_7C_9)$	-164.3(9)	-165.7(10)	-165.7	-165.9	-168.0(9)	165.3(6)	-165.3(8)
$\angle(C_4C_5C_7C_8)$	-39.3(7)	-39.6(8)	-38.6	-38.8	-40.3(7)	-37.2(7)	-36.0(7)
$\angle(C_{10}C_2C_3C_4)$	150.7(3)	150.5(5)	149.7	150.5	177.8(13)	155.8(8)	–
$\angle(C_{10}C_1C_2C_3)$	154.9(9)	152.5(14)	152.0	152.5	179.1(35)	179.5(5)	–
$\angle(C_3OC_2C_1)$	-107.0(7)	-104.5(7)	-103.7	-104.0	–	–	–
$\sigma_{fit}/(uÅ^2)$	–	0.0088	–	–	0.0087	0.0080	0.0079

[a] Ref. [15]; [b] Ref. [16]; [c] calculated using 6-311++G(d,p) basis set.

Conclusions

The broadband rotational spectra of α-pinene oxide has been recorded using the Lille CP-FTMW spectrometer in the 6-18 GHz range. ^{13}C and ^{18}O isotopologues were observed in their natural abundances allowing the determination of an experimental structure of the heavy atom skeleton using the ground-state (r_0) substitution (r_s) methods. Theoretical calculations using density functional and *ab initio* methods have been performed to obtain the equilibrium structure, and to guide the spectral analysis.

The gas-phase structure of APO has been compared to related molecules such as α-pinene, β-pinene and nopinone. Their structures were found to be very similar in particular between α-pinene oxide and α-pinene. As in the case of β-pinene/nopinone, the oxidation of α-pinene does not affect too much the structure even with the formation of a tricyclic APO molecule the main structural difference involves the dihedral angle $C_{10}C_1C_2C_3$. With the β-pinene and nopinone more structural features could be observed and mainly in the dihedral angles $C_2C_3C_4C_5$, $C_4C_3C_2C_1$, $C_3C_4C_5C_7$, $C_3C_4C_5C_6$ and $C_3C_4C_5C_7$. Those structural changes are associated with the presence of epoxide functional group, which tilts the five ring atoms.

SUPPLEMENTARY MATERIAL

The Supplementary Material contains calculated parameters of the APO at MP2/6-311++G(d,p), the fitted lines for the main species and monosubstituted isotopologues of APO. It contains also the obtained coordinates, r_s, and their associated uncertainties.

Conflicts of interest

There are no conflicts to declare

Acknowledgements

The present work was funded by the French ANR Labex CaPPA through the PIA under contract ANR-11-LABX-0005-01, by the Regional Council Hauts-de-France and by the European Funds for Regional Economic Development (FEDER), and by the CPER CLIMIBIO and CPER P4S. E. M. N. would like to thank the CNRS for a researcher contract.

References

[1] A.B. Guenther, X. Jiang, C.L. Heald, T. Sakulyanontvittaya, T. Duhl, L.K. Emmons, and X. Wang, Geosci. Model Dev. **5**, 1471 (2012).

[2] J.-F. Müller, T. Stavrakou, S. Wallens, I. De Smedt, M. Van Roozendael, M.J. Potosnak, J. Rinne, B. Munger, A. Goldstein, and A.B. Guenther, Atmos. Chem. Phys. **8**, 1329 (2008).

[3] S. Fuzzi, U. Baltensperger, K. Carslaw, S. Decesari, H. Denier Van Der Gon, M.C. Facchini, D. Fowler, I. Koren, B. Langford, U. Lohmann, E. Nemitz, S. Pandis, I. Riipinen, Y. Rudich, M. Schaap, J.G. Slowik, D. V Spracklen, E. Vignati, M. Wild, M. Williams, and S. Gilardoni, Atmos. Chem. Phys **15**, 8217 (2015).

[4] M. Kanakidou, J.H. Seinfeld, S.N. Pandis, I. Barnes, F.J. Dentener, M.C. Facchini, R. Van Dingenen, B. Ervens, A. Nenes, C.J. Nielsen, E. Swietlicki, J.P. Putaud, Y. Balkanski, S. Fuzzi, J. Horth, G.K. Moortgat, R. Winterhalter, C.E.L. Myhre, K. Tsigaridis, E. Vignati, E.G. Stephanou, and J. Wilson, *Organic Aerosol and Global Climate Modelling: A Review* (2005).

[5] R. Zhang, Science **328**, 1366 (2010).

[6] J. Lelieveld, T.M. Butler, J.N. Crowley, T.J. Dillon, H. Fischer, L. Ganzeveld, H. Harder, M.G. Lawrence, M. Martinez, D. Taraborrelli, and J. Williams, Nature **452**, 737 (2008).

[7] M. Hallquist, J.C. Wenger, U. Baltensperger, Y. Rudich, D. Simpson, M. Claeys, J. Dommen, N.M. Donahue, C. George, A.H. Goldstein, J.F. Hamilton, H. Herrmann, T. Hoffmann, Y. Iinuma, M. Jang, M.E. Jenkin, J.L. Jimenez, A. Kiendler-Scharr, W. Maenhaut, G. McFiggans, T.F. Mentel, A. Monod, A.S.H. Prévôt, J.H. Seinfeld, J.D. Surratt, R. Szmigielski, and J. Wildt, Atmos. Chem. Phys. **9**, 5155 (2009).

[8] R.J. Griffin, D.R. Cocker, J.H. Seinfeld, and D. Dabdub, Geophys. Res. Lett. **26**, 2721 (1999).

[9] Y. Yu, M.J. Ezell, A. Zelenyuk, D. Imre, L. Alexander, J. Ortega, J.L. Thomas, K. Gogna, D.J. Tobias, B. D'Anna, C.W. Harmon, S.N. Johnson, and B.J. Finlayson-Pitts, Phys. Chem. Chem. Phys. **10**, 3063 (2008).

[10] Y. Yu, M.J. Ezell, A. Zelenyuk, D. Imre, L. Alexander, J. Ortega, B. D'Anna, C.W. Harmon, S.N. Johnson, and B.J. Finlayson-Pitts, Atmos. Environ. **42**, 5044 (2008).

[11] T. Berndt, O. Böge, and F. Stratmann, Atmos. Environ. **37**, 3933 (2003).

[12] Y. Iinuma, O. Böge, A. Kahnt, and H. Herrmann, Phys. Chem. Chem. Phys. **11**, 7985 (2009).

[13] A.S. Singh, D.R. Naikwadi, K. Ravi, and A. V. Biradar, Mol. Catal. **521**, 112189 (2022).

[14] C.J. Ribeiro, M.M. Pereira, E.F. Kozhevnikova, I. V Kozhevnikov, E. V Gusevskaya, and K.A. da Silva Rocha, Catal. Today **344**, 166 (2020).

[15] E.M. Neeman, J.R. Avilés Moreno, and T.R. Huet, J. Chem. Phys. **147**, 214305 (2017).

[16] E.M. Neeman, J.R. Avilés-Moreno, and T.R. Huet, Phys. Chem. Chem. Phys. **19**, 13819 (2017).

[17] C. Medcraft and M. Schnell, Zeitschrift Fur Phys. Chemie **230**, 1 (2016).

[18] E.M. Neeman, P. Dréan, and T.R. Huet, J. Mol. Spectrosc. **322**, 50 (2016).

[19] E.M. Neeman, N. Osseiran, and T.R. Huet, J. Chem. Phys. **156**, 124301 (2022).

[20] G.G. Brown, B.C. Dian, K.O. Douglass, S.M. Geyer, S.T. Shipman, and B.H. Pate, Rev. Sci. Instrum. **79**, 053103 (2008).

[21] G.G. Brown, B.C. Dian, K.O. Douglass, S.M. Geyer, and B.H. Pate, J. Mol. Spectrosc. **238**, 200 (2006).

[22] M.J. Frisch, G.W. Trucks, H.B. Schlegel, G.E. Scuseria, M.A. Robb, J.R. Cheeseman, G. Scalmani, V. Barone, G.A. Petersson, H. Nakatsuji, X. Li, M. Caricato, A. V. Marenich, J. Bloino, B.G. Janesko, R. Gomperts, B. Mennucci, H.P. Hratchian, J. V. Ortiz, A.F. Izmaylov, J.L. Sonnenberg, D. Williams-Young, F. Ding, F. Lipparini, F. Egidi, J. Goings, B. Peng, A. Petrone, T. Henderson, D. Ranasinghe, V.G. Zakrzewski, J. Gao, N. Rega, G. Zheng, W. Liang, M. Hada, M. Ehara, K. Toyota, R. Fukuda, J. Hasegawa, M. Ishida, T. Nakajima, Y. Honda, O. Kitao, H. Nakai, T. Vreven, K. Throssell, J.A. Montgomery, Jr., J.E. Peralta, F. Ogliaro, M.J. Bearpark, J.J. Heyd, E.N. Brothers, K.N. Kudin, V.N. Staroverov, T.A. Keith, R. Kobayashi, J. Normand, K. Raghavachari, A.P. Rendell, J.C. Burant, S.S. Iyengar, J. Tomasi, M. Cossi, J.M. Millam, M. Klene, C. Adamo, R. Cammi, J.W. Ochterski, R.L. Martin, K. Morokuma, O. Farkas, J.B. Foresman, and D.J. Fox, Gaussian 16, Rev. C. 01 Gaussian Inc. (2016).

[23] C. Møller and M.S. Plesset, Phys. Rev. **46**, 618 (1934).

[24] A.D. Becke, J. Chem. Phys. **98**, 5648 (1993).

[25] C. Lee, W. Yang, and R.G. Parr, Phys. Rev. B **37**, 785 (1988).

[26] Y. Zhao and D.G. Truhlar, Theor. Chem. Acc. **120**, 215 (2008).

[27] J. Wu, L.G. Gao, Z. Varga, X. Xu, W. Ren, and D.G. Truhlar, Angew. Chemie Int. Ed. **59**, 10826 (2020).

[28] L.A. Curtiss, K. Raghavach Ari, P.C. Redfern, V. Rassolov, and J.A. Pople, J. Chem. Phys. **109**, 7764 (1998).

[29] N. Osseiran, E.M. Neeman, M. Goubet, H. Damart, G. Dekyndt, and T.R. Huet, in *26th Int. Conf. High Resolut. Mol. Spectrosc.* (2022), pp. K5, p160.

[30] M. Tudorie, L.H. Coudert, T.R. Huet, D. Jegouso, and G. Sedes, J. Chem. Phys. **134**, 074314 (2011).

[31] H.M. Pickett, J. Mol. Spectrosc. **148**, 371 (1991).

[32] J.K.G. Watson, in *Vib. Spectra Struct. Vol.6. A Ser. Adv.* (1977), pp. 1–89.

[33] J. Kraitchman, Am. J. Phys. **21**, 17 (1953).

[34] C.C. Costain, Trans. Am. Cryst. Assoc. **2**, 157 (1966).

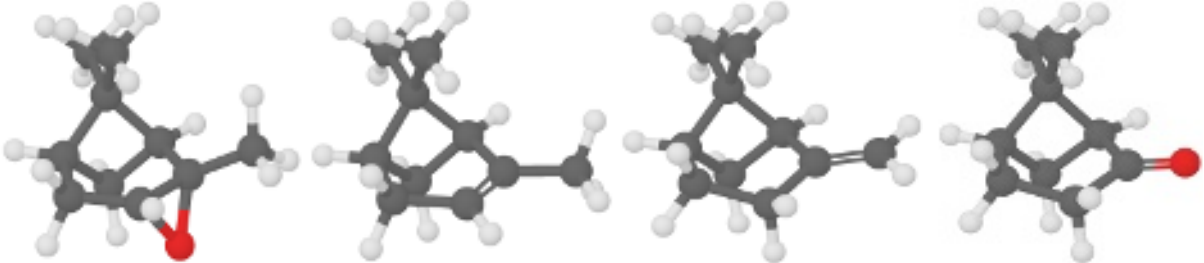

α-pinene oxide α-pinene β-pinene nopinone

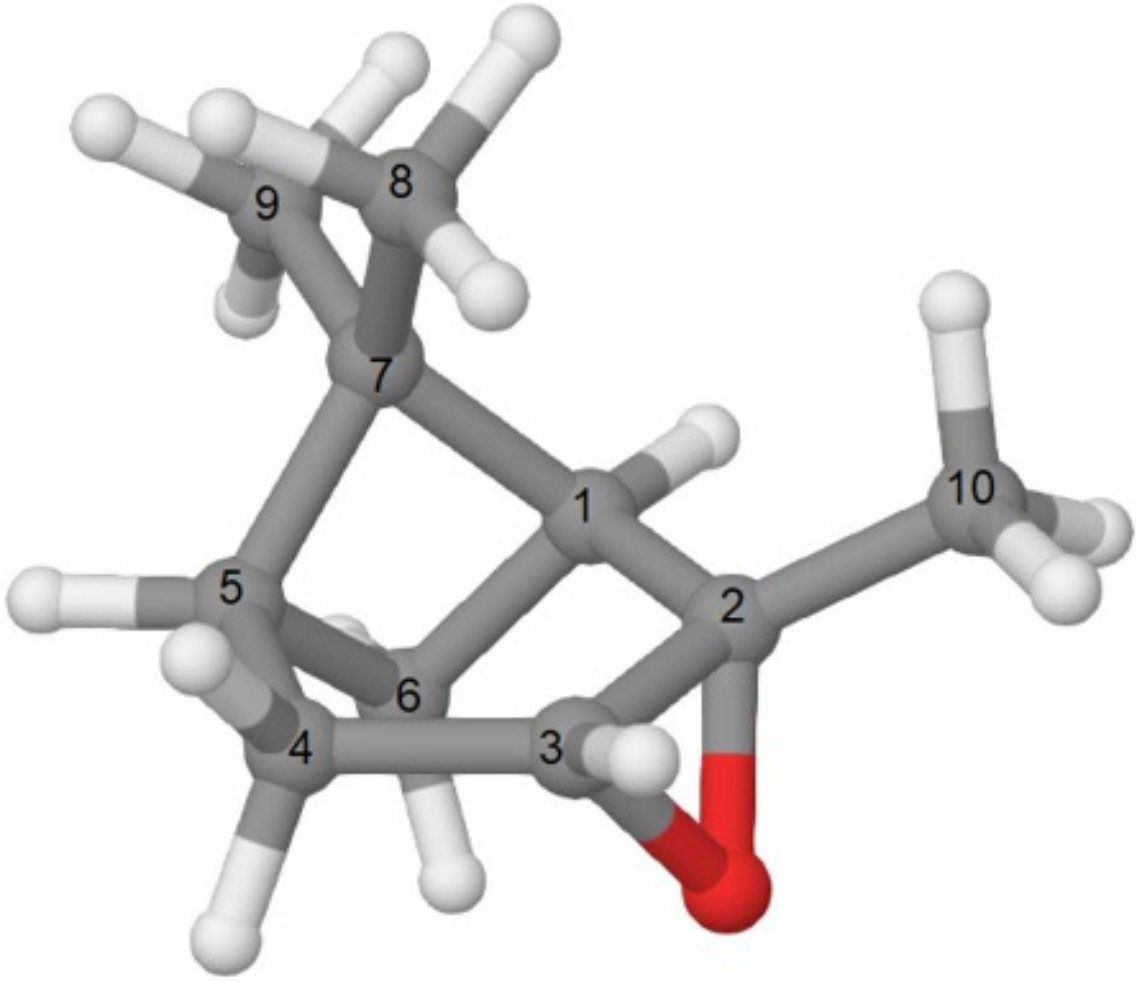

apo-I

$\Delta E = 0$ kJ.mol^{-1}

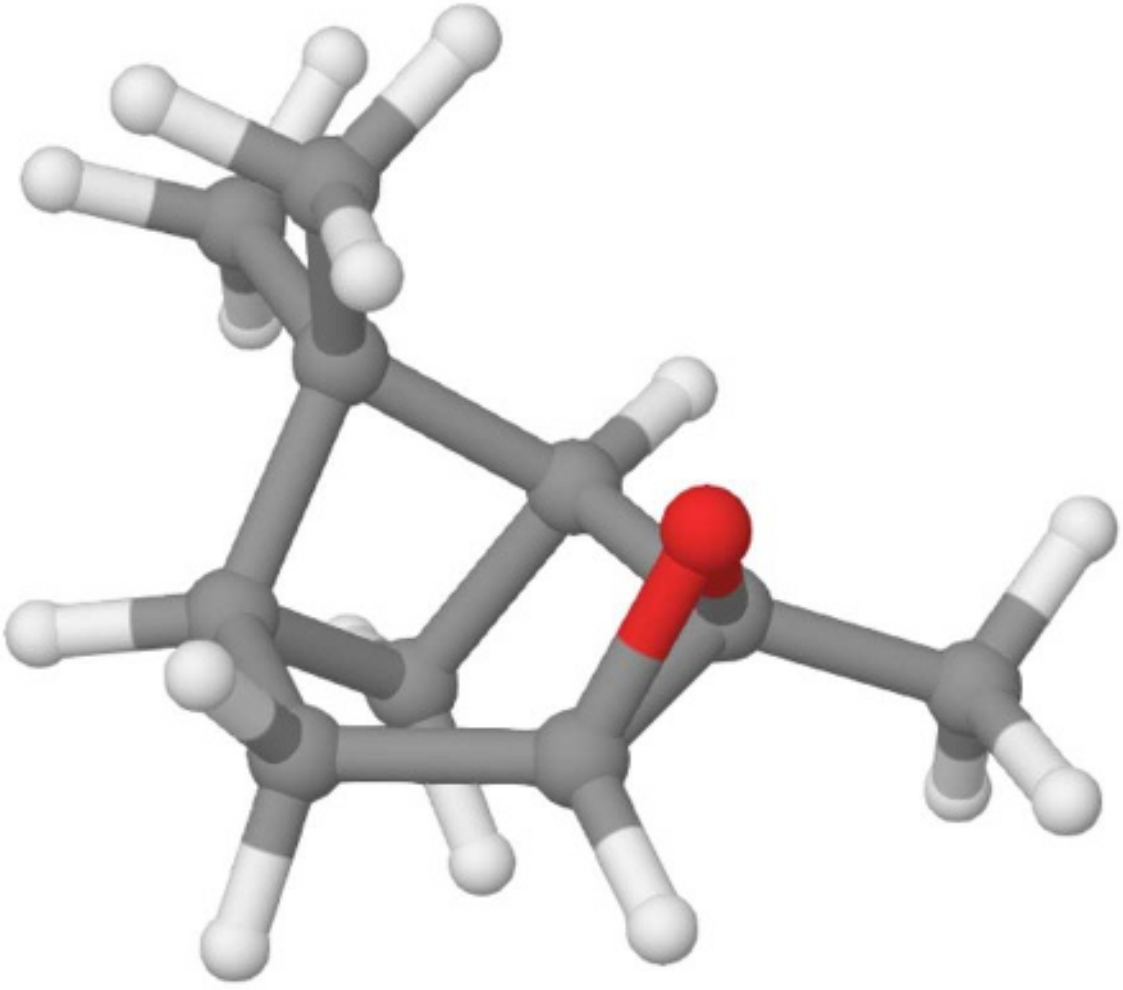

apo-II

$\Delta E = 18; 18; 15; 20$ kJ.mol^{-1}

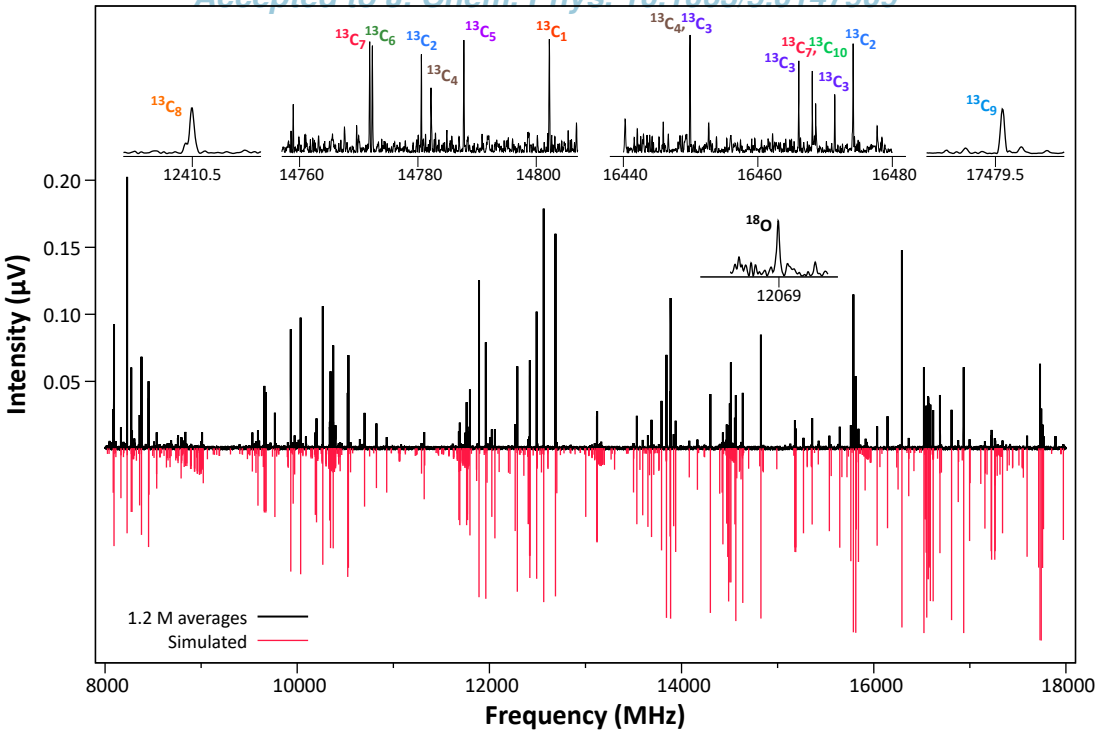

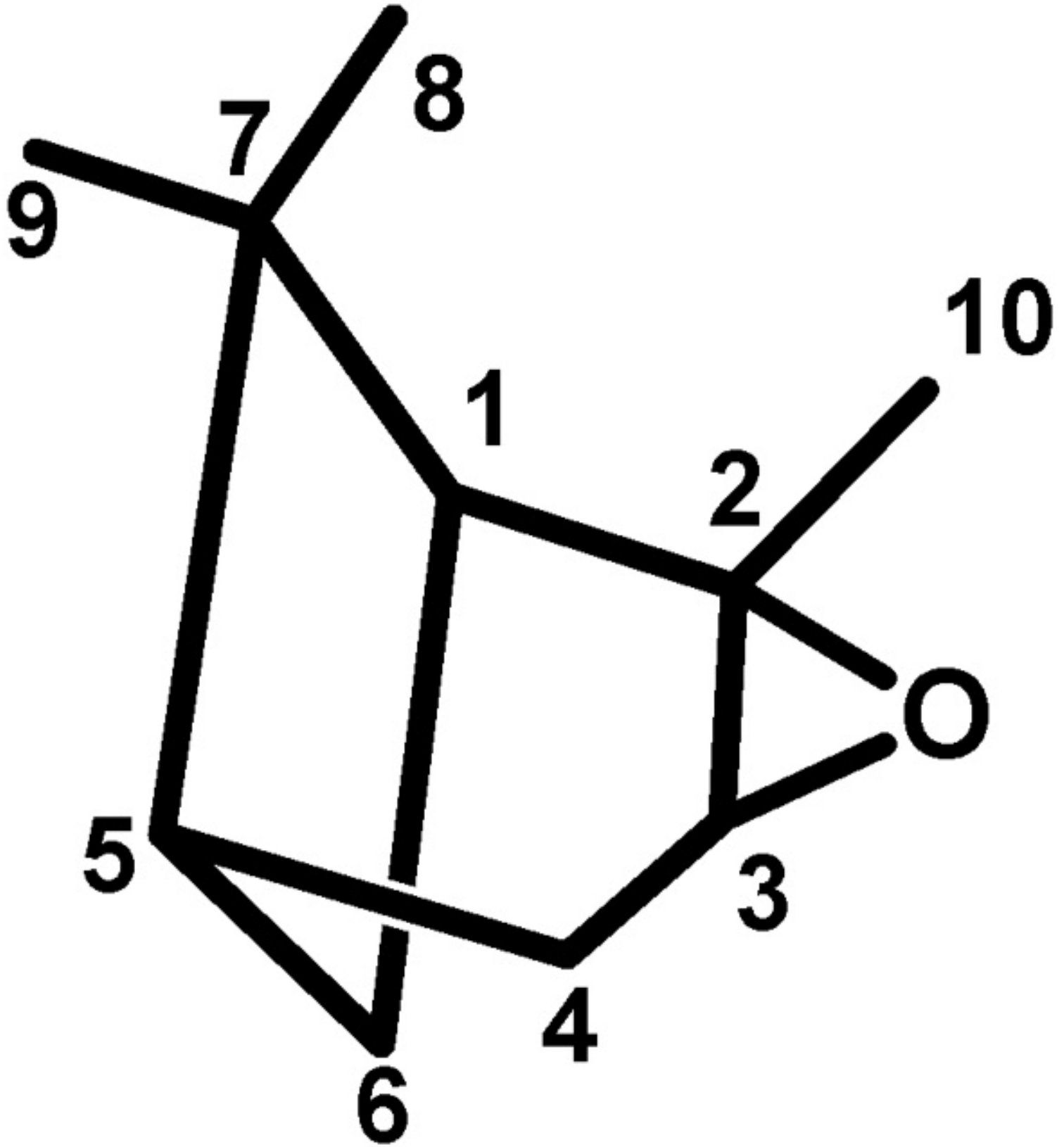
8
7
9
10
1
2
O
5
3
4
6

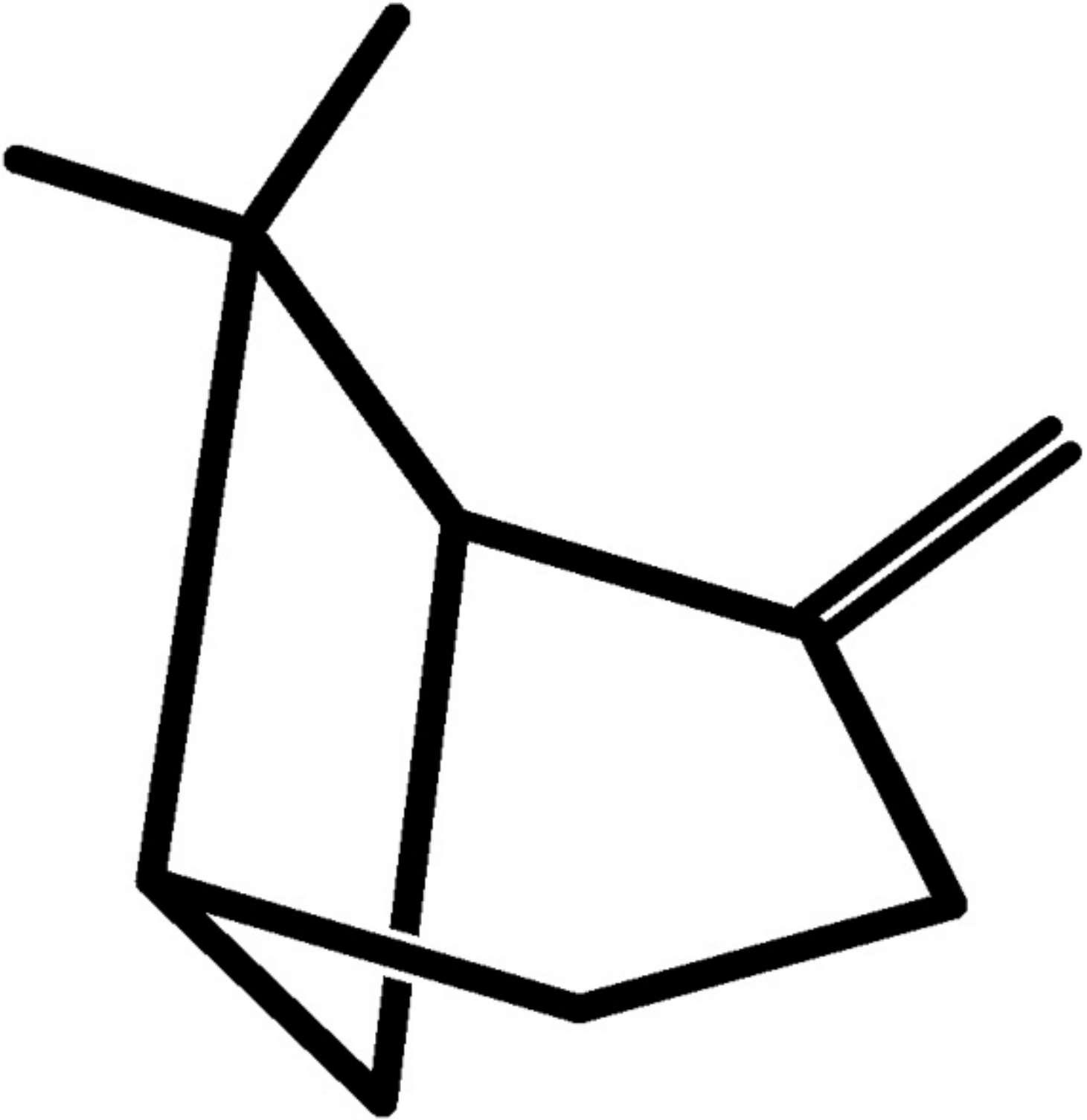

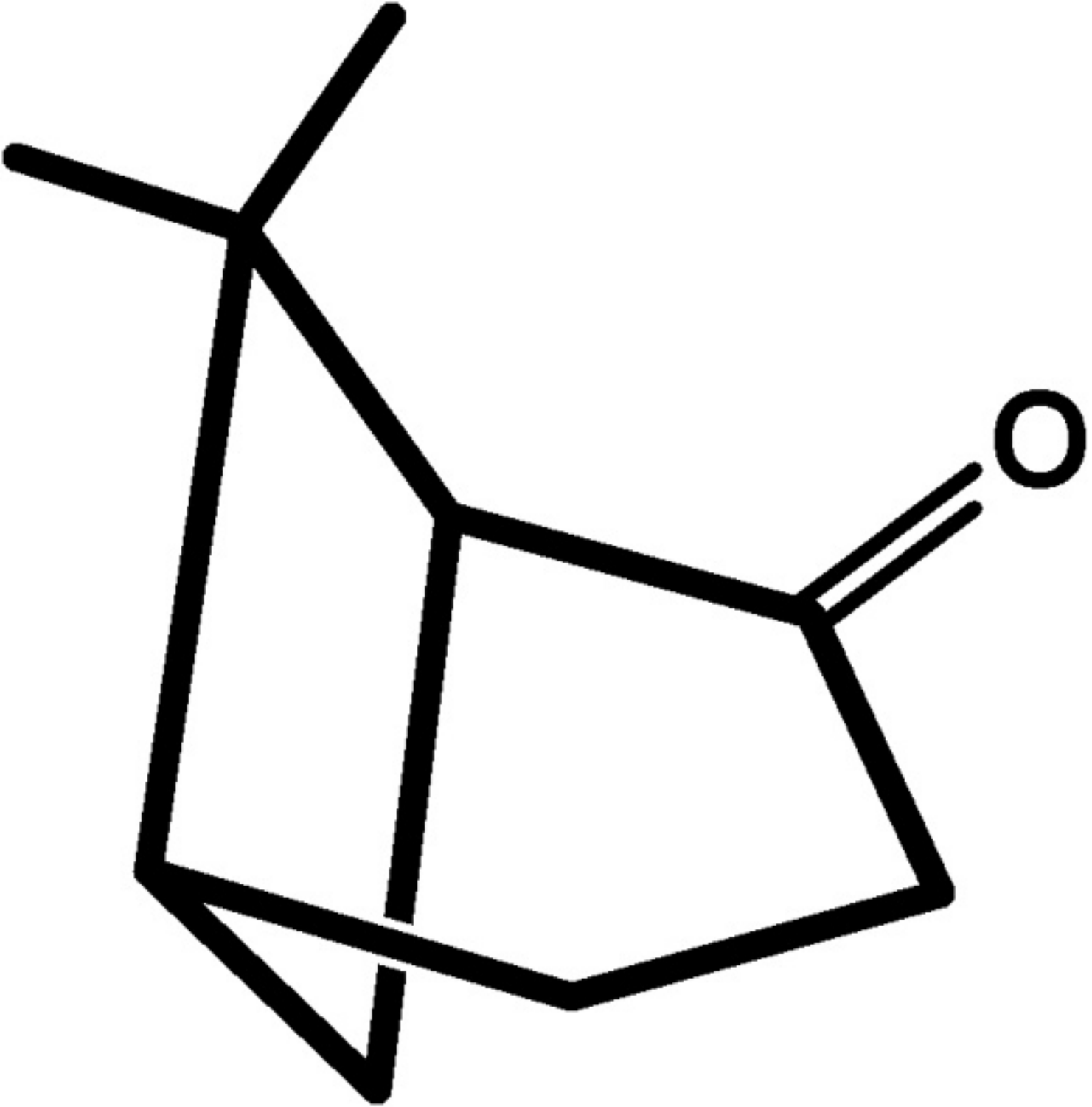
O